

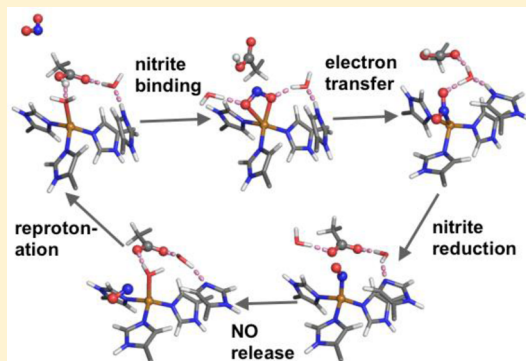
## Enzymatic Mechanism of Copper-Containing Nitrite Reductase

Yan Li, Miroslav Hodak,\* and J. Bernholc\*

Center for High Performance Simulation and Department of Physics, North Carolina State University, Raleigh, North Carolina 27695-7518, United States

### Supporting Information

**ABSTRACT:** Copper-containing nitrite reductases (CuNiRs) catalyze the reduction of nitrite to nitric oxide, a key step in the denitrification process that maintains balance between organic and inorganic nitrogen. Despite their importance, their functioning is not well understood. In this work, we carry out first-principles calculations and show that the available structural data are consistent only with a single mechanism. For this mechanism, we determine the activation energies, transition states, and minimum energy pathways of CuNiR. The calculations lead to an updated enzymatic mechanism and resolve several controversial issues. In particular, our work identifies the origins of the two protons necessary for the enzymatic function and shows that the transformation from the initial O-coordination of substrate to the final N-coordination of product is achieved by electron transfer from T1 copper to T2 copper, rather than by the previously reported side-on coordination of a NO intermediate, which only takes place in the reduced enzyme. We also examine the role of structural change in the critical residue Asp<sup>98</sup>, reported in one experimental study, and find that while the structural change affects the energetics of substrate attachment and product release at the T2 copper reaction center, it does not significantly affect the activation energy and reaction pathways of the nitrite reduction process.



The nitrogen cycle is a process in which nitrogen is converted between biological and nonbiological forms. The two important stages of this process are nitrogen fixation and denitrification. The former converts atmospheric nitrogen into biological forms, while the latter releases biological nitrogen back into the atmosphere in the form of N<sub>2</sub>. Historically, denitrification balanced nitrogen fixation, making the amount of nitrogen in the atmosphere, soil, and aquatic ecosystems stable. However, human activity has altered the balance since the discovery of the Haber-Bosch process, which enables an inexpensive way of fixing atmospheric nitrogen into ammonia for production of fertilizers. As a result, the rate of nitrogen input into the terrestrial and aquatic ecosystems has doubled<sup>1</sup> and is still increasing due to the use of synthetic fertilizers and cultivation of nitrogen-fixing crops. The excess nitrogen causes many environmental problems, especially in aquatic ecosystems such as eutrophication and harmful algal blooms. Denitrification<sup>2,3</sup> is currently the only proven nitrogen removal process, which transforms biological nitrate (NO<sub>3</sub><sup>-</sup>) into N<sub>2</sub> gas. This anoxic process occurs in four reduction steps: initial conversion of nitrate to nitrite (NO<sub>3</sub><sup>-</sup> → NO<sub>2</sub><sup>-</sup>), followed by transformation of nitrite to nitric oxide (NO<sub>2</sub><sup>-</sup> → NO), subsequent reduction of nitric oxide to nitrous oxide (NO → N<sub>2</sub>O), and the final conversion of nitrous oxide to dinitrogen gas (N<sub>2</sub>O → N<sub>2</sub>). All stages are catalyzed by complex metalloenzymes with different transition metal cofactors. To remediate human impact on the environment, it is necessary to fully understand the mechanisms of metalloenzymes involved in this process.

Dissimilatory nitrite reductases (NiRs) catalyze the reduction of nitrite to nitric oxide, the committed step in denitrification. There are two main types: one containing iron (cd<sub>1</sub>NiRs) and the other copper (CuNiRs). cd<sub>1</sub>NiRs started to occur at an early evolutionary stage of NiR history. As the amount of O<sub>2</sub> in atmosphere increased, more and more CuNiRs were found. The mechanism of heme cd<sub>1</sub> nitrite reductases is by now well-known,<sup>4</sup> while the functioning of CuNiRs is not well understood. The CuNiRs are organized as homotrimers with three identical monomers tightly associated together.<sup>5-7</sup> Each monomer contains two copper sites: type I (T1) and type II (T2), which are connected via a cysteine (Cys)-histidine (His) bridge for rapid electron transfer as shown in Figure 1. The T1 copper, which is the site of electron transfer from a physiological electron donor, is coordinated by two histidine imidazoles, one cysteine thiolate, and one methionine thioether. The T2 copper, which is the site of nitrite reduction, is coordinated by three histidine imidazoles and a water molecule in the resting state.<sup>8,9</sup> Experiments<sup>8,9</sup> on native nitrite-soaked CuNiRs revealed that nitrite binds in a bidentate mode via two oxygen atoms and forms a hydrogen bond with Asp<sup>98</sup>, which connects to His<sup>255</sup> through a solvent-bridged hydrogen bond. The conserved active site, hydrophobic residue Ile<sup>257</sup>, positioned within 3 Å from the bound substrate and product,

Received: June 23, 2014

Revised: December 11, 2014

Published: January 16, 2015



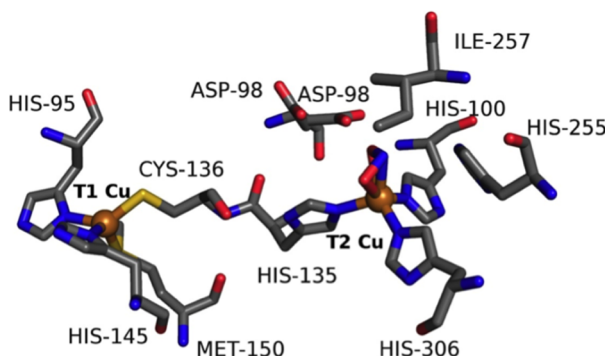


**Figure 1.** T1 and T2 copper sites with nearby residues (PDB ID 2BWD). T2 is the catalytic site, while the T1 copper transfers an external electron to the T2 copper during the catalytic process.

has been found to shape the active site cavity and limit inhibition of CuNiR by small molecules.<sup>10</sup>

The catalytic mechanism of CuNiR has been investigated in crystallographic,<sup>9,11–14</sup> spectroscopic,<sup>15–17</sup> kinetic and mutational studies<sup>9,18–21</sup> of enzymes from different species. Asp<sup>98</sup> and His<sup>255</sup> mutants show a decrease in the reaction rate constant, proving that these residues are critical for enzymatic function of CuNiR.<sup>9,18–21</sup> Other studies have further elucidated the role of Asp<sup>98</sup> and His<sup>255</sup> in CuNiRs: X-ray experiments<sup>9,11–14</sup> revealed that the Asp<sup>98</sup> forms a hydrogen bond to both the nitrite substrate and the nitric oxide product and that this residue is critical for proton transfer during catalysis. In the same studies, His<sup>255</sup> was proposed to participate in proton transfer to a catalytic intermediate either directly or via Asp<sup>98</sup>.

Although these works have provided a great deal of insight into the mechanism of CuNiR, several important questions remain unanswered. One of them is a change of coordination at the T2 Cu site, where the substrate is initially O-coordinated, while the product ends up in an N-coordinated mode. A key insight into this can be obtained from the structure of the NO intermediate, but attempts to detect it directly during the reaction have not been successful yet. Instead, a couple of experiments<sup>11,12</sup> were able to detect the structure of the CuNiR-NO complex by exposing the crystallized enzyme in its reduced form to NO solution. These studies found that the NO molecule attaches in a symmetric “side-on” way, in which Cu–N and Cu–O bond lengths are approximately equal. These findings were unexpected, since NO is usually N-coordinated in Cu complexes, and have generated multiple follow-up studies,<sup>22–26</sup> because a side-on structure of the NO intermediate would have important consequences for the enzymatic action of CuNiR. While it was determined that the side-on binding is promoted by a hydrogen bond with Asp<sup>98</sup> along with interaction with Ile<sup>257</sup> and His<sup>255</sup>, it is still unknown whether it takes place during the enzymatic action, as CuNiR is oxidized rather than reduced when NO attaches.

Interestingly, one of the studies<sup>12</sup> addressing the NO intermediate has found that one of the key residues, Asp<sup>98</sup>, changes side-chain conformation according to the attachment of the substrate, suggesting an additional role of this residue. In the “gatekeeper” position, which takes place in the nitrite-bound state, the carboxyl group is oriented toward the substrate entry pocket, while in the “proximal” position, which was detected in the resting enzyme, the carboxyl group points to the proton channel and is close to the reaction center.

Another unresolved issue is the origin of the two protons that are required for CuNiR’s enzymatic action. The fact that X-ray experiments, which have been used to explore the structure of this enzyme, cannot detect protons, means that this aspect of its mechanism remains unexplored. Similarly, the transformation from the initial O-coordinated nitrite to the final N-coordinated nitric oxide remains unclear.

So far, multiple theoretical studies have addressed the binding mode of NO and nitrite at the T2 copper site. The side-on binding mode of NO at reduced Cu(I) site was found to be promoted by the hydrogen bond with Asp<sup>98</sup> along with interactions with Ile<sup>257</sup> and His<sup>255</sup>.<sup>22–26</sup> By combining computational models with experimental spectroscopic technique, Ghosh and co-workers found that the bidentate coordination mode of nitrite occurs when either or both of Asp<sup>98</sup> and His<sup>255</sup> are protonated. Other theoretical studies showed that protonated nitrite (HNO<sub>2</sub>) at oxidized Cu(II) is energetically unstable and decays to generate damaging NO<sup>+</sup>. Although these works provide a great deal of insight into the mechanism of CuNiR, many important questions remain unanswered: (1) Does the side-on coordination of NO occur at oxidized Cu(II)? (2) How does the initial O-coordinated nitrite proceed to the final N-coordinated NO? (3) Does the conformation of Asp<sup>98</sup> play a role in the reaction? (4) What are the origins of the protons?

In this paper, we investigate CuNiR enzymatic function using density functional theory.<sup>27,28</sup> We employ the nudged elastic band (NEB)<sup>29,30</sup> method to determine minimum energy pathways (MEPs), transition states, and activation energies for the steps in enzymatic conversion of nitrite to nitric oxide. To our knowledge, there has been so far only one transition state calculation of the CuNiR function,<sup>31</sup> which used saddle point optimization that requires a very good initial guess of the transition states. Our NEB calculations give precise minimum energy pathways, transition states and accurate activation energies, providing a clear picture of the entire enzymatic process. Our calculations also resolve a number of issues. First, we find that flexibility of the Asp<sup>98</sup> side chain reported in one of the experimental studies<sup>12</sup> can stabilize the attachment of the substrate as well as the release of the product. We also identify the origins of the two protons participating in the catalytic reaction: one comes from Asp<sup>98</sup>, while the other is transferred from His<sup>255</sup> via a water bridge. Furthermore, while the side-on coordination of the copper-nitrosyl is a local minimum on the energy landscape, the end-on coordination is an even lower minimum. Finally, the calculations suggest that the different oxidation states of the copper sites play important roles in the transformation from the O-coordination of nitrite to the N-coordination of nitric oxide.

## MATERIALS AND METHODS

Our model of the CuNiR active site is based on the reported structure of CuNiR from *Achromobacter cycloclastes* (PDB codes 2BWI, 2BWS, 2BWD)<sup>12</sup> and consists of the following residues: His<sup>100</sup>, His<sup>135</sup>, His<sup>306</sup>, Asp<sup>98</sup>, His<sup>255</sup>, Ile<sup>257</sup>, and four nearby water molecules, resulting in a total of 105 atoms as displayed in Figure 2. This model is relatively small because the NEB calculations are computationally demanding, but it is in close agreement with experimental data. A comparison to a larger model (a total of 180 atoms) shows that the structural parameters at the active copper site differ by less than 1%. In the calculations, the coordinates of the alpha carbons of each

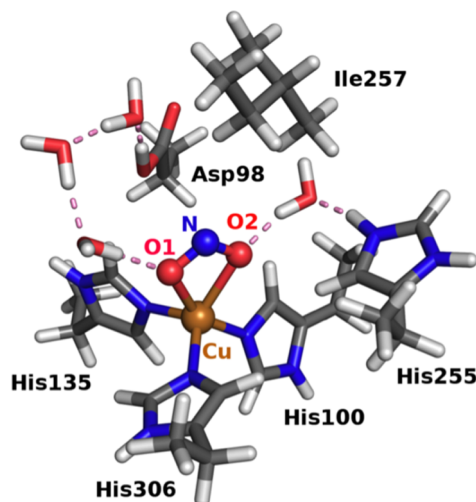


**Figure 2.** Computational model consists of His<sup>100</sup>, His<sup>135</sup>, His<sup>306</sup>, Asp<sup>98</sup>, His<sup>255</sup>, Ile<sup>257</sup>, and four water molecules. In the calculations, alpha carbons in each protein fragment are fixed to their experimental positions.

residue are frozen to their experimental positions. All the other atoms, including those in water molecules, are free to move.

The calculations are based on density functional theory (DFT), which has many applications to biological systems and has been successful in understanding many complex enzyme reaction pathways at a molecular level.<sup>32–35</sup> We use both the Real-Space Multigrid (RMG)<sup>36–38</sup> and Quantum Espresso (QE)<sup>39</sup> codes for structural optimization with the PBE XC functional and ultrasoft pseudopotentials. The QE calculations use kinetic energy cutoff of 30 Ry, while RMG calculations use a grid spacing of 0.32 Bohr.

To investigate the catalytic function of CuNiR, we use the NEB method, which searches for the minimum energy pathway between specified initial and final states and thus also provides the energy barrier for the process. In NEB calculations, the investigated process is divided into several steps along the pathway between the initial and final states. An important advantage of the NEB approach is that calculations corresponding to each step, called “images”, can be run in parallel with only infrequent checkpoints, which make NEB ideal for use on massively parallel supercomputers. Saddle point calculations are often used to explore catalytic processes, but these require a good initial guess of the saddle point state and do not provide full reaction pathways.

Here, we use the climbing-image nudged elastic band (CI-NEB) method,<sup>29,30</sup> as implemented in the Quantum Espresso code, which improves on the standard NEB method by using a

special treatment for the highest energy image to ensure that it is driven up to the saddle point. The convergence criteria in our NEB calculations are that atomic forces of all images must be less than 0.05 eV/Å. The calculations are carried out on a Cray XE6 supercomputer and use nine images in an NEB simulation with each image using 110 CPU cores. The entire catalytic process is studied in three steps, with separate NEB calculations corresponding to substrate attachment, nitrite reduction, and product release, respectively. All three simulations are run concurrently, and a total of 2970 cores is used.

The channels leading to and from the T2 Cu site are found by using the CAVER<sup>40</sup> plugin to molecular visualization software PyMol.<sup>41</sup> CAVER is a software tool for analysis and visualization of channels in protein structures. In CAVER, the most accessible channel from the protein cavity to the bulk solvent is found by minimizing the sum of the cost function for all nodes of the channel. The cost function is inversely proportional to the square of the distance between the node and the protein. The initial position of NO<sub>2</sub><sup>–</sup> before the attachment and the final position of NO after release for the NEB calculations are determined by confining the molecules inside the channel and optimizing the geometries.

## RESULTS

**Energetics at Two Positions of Asp<sup>98</sup>.** In the X-ray experiment by Antonyuk and co-workers,<sup>12</sup> two conformations of Asp<sup>98</sup> side chain were found. They named them gatekeeper and proximal: the former is close to the substrate entry pocket, while the latter is close to the T2 copper center. The experiment could not determine under what conditions the conformation change occurs or whether it plays a role in the enzymatic function. It should be noted that ref 12 is the only experimental work that found conformational change in Asp<sup>98</sup>. However, because this residue is directly involved in the NO<sub>2</sub><sup>–</sup> to NO conversion process, we include its conformational change in our calculations to determine if it has an effect on the enzymatic function.

We examined channels leading to the catalytic site using CAVER.<sup>40</sup> The two channels with largest bottleneck radii are displayed in Figure 3A. The larger one with the bottleneck diameter is 3.12 Å and thus can fit both the substrate and the product—the O–O distance in NO<sub>2</sub><sup>–</sup> is 2.11 Å, while the N–O bond length in NO is 1.15 Å. The smaller channel can only fit the product, as its bottleneck diameter is 2.08 Å. The two channels coincide close to the reaction center. Detailed views of the channels are provided in Figure S7 (SI).

The two positions of the Asp<sup>98</sup> side chain relative to the channels are displayed in Figure 3B,C, where the green side-chain is in the “gatekeeper” position pointing toward the nitrite-

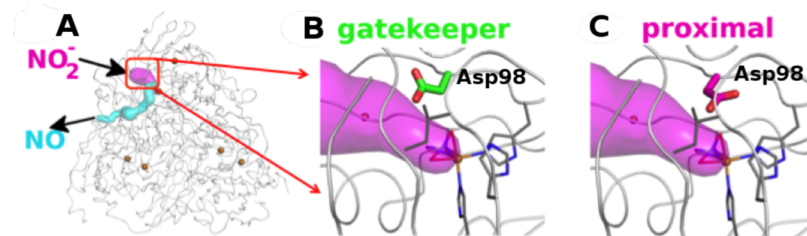


**Figure 3.** Channels connecting the outside of the enzyme to the T2 Cu site. The experimental structure is from PDB ID code 2BWD (NO + NO<sub>2</sub><sup>–</sup>). (A) Two largest channels in the enzyme, shown in pink (the larger one) and blue (the smaller one), respectively. (B) Asp<sup>98</sup> side chain in the gatekeeper position. (C) Asp<sup>98</sup> side chain in the proximal position.

binding channel, while the pink side chain is in the “proximal” position that is close to the active site.

Our CAVER analysis shows that the “proximal” conformation is preferable in the resting state to facilitate the subsequent nitrite attachment. It has a shorter length, a lower average cost to navigate the channel as well as weaker steric interactions with the nitrite.

We have investigated the energetic competition between the “gatekeeper” and “proximal” positions at multiple stages of the catalytic process. The results are summarized in Table 1, and

**Table 1. Energy Comparisons between the “Gatekeeper” and “Proximal” Conformations**

T2 Cu site	favorable conformation	$E_{\text{favorable}} - E_{\text{unfavorable}}$ (kcal/mol)
$\text{NO}_2^-$ -Cu(II) <sup>a</sup>	gatekeeper	-8.07
$\text{NO}_2^-$ -Cu(I) <sup>a</sup>	gatekeeper	-8.76
$\text{NO}$ -Cu(II) <sup>b</sup>	proximal	-5.53
$\text{H}_2\text{O}$ -Cu(II) <sup>b</sup>	proximal	-4.38

<sup>a</sup>His<sup>255</sup> and Asp<sup>98</sup> are protonated. <sup>b</sup>His<sup>255</sup> and Asp<sup>98</sup> are deprotonated.

the optimized structures of the preferred conformations are shown in Figure 4. All optimized structures including the unfavorable ones are shown in Figure S6 (SI) with distances between Cu and nitrite/NO/water displayed. We find that the “gatekeeper” position is favored for the substrate-bound state (Figure 4A) and remains such even after ET and reduction of the Cu center (Figure 4B). However, after nitrite reduction,

“proximal” position becomes preferable (Figure 4C). This configuration does not change after the product is released (Figure 4D). These results suggest that Asp<sup>98</sup> is in the “proximal” position in the enzyme resting state, but it moves to the “gatekeeper” conformation upon substrate attachment to facilitate attachment of the nitrite. During nitrite reduction, Asp<sup>98</sup> moves back to the “proximal” position. This is consistent with our CAVER analysis, which showed that the “gatekeeper” conformation is preferable for nitrite attachment. These findings are also in agreement with X-ray experiments by Antonyuk and co-workers,<sup>12</sup> which showed that the “proximal” conformation of Asp<sup>98</sup> is more pronounced in the electron density map when nitrite binds to copper, while the “proximal” confirmation is preferred when water or nitric oxide bind to copper.

One difference, when compared to the experimental structures, is the position of the nitrite when attached to the oxidized enzyme. Experiments<sup>12</sup> find a face-on coordination (experimental distances in Å: O1—Cu=2.04, O2—Cu=2.29, and N—Cu=2.36), while we find a bidentate O-coordination with the nitrogen pointing away from the copper (calculated distances in Å: O1—Cu=2.13, O2—Cu=2.27, and N—Cu=2.65, see Figure S6 for details). Comparisons between the experimental and calculated structures are shown in Figure S1 (SI). Interestingly, the calculated bidentate coordination of nitrite-Cu(II), as displayed in Figure 4A, agrees with Sundararajan’s DFT calculations,<sup>24</sup> in which the nitrogen is also pointing away from the copper.

For the reduced form of Cu(I)-nitrite, no experimental structures are available. To get an optimized structure of Cu(I)-nitrite, there are two common approaches to choose a starting point: one is to start with the experimental structure of the oxidized form; the other is to start with a computationally optimized structure of the oxidized form. In this paper, we started with the experimental nitrite-Cu(II) configuration. After adding one electron to reduce Cu(II) to Cu(I), we obtained an optimized structure of nitrite-Cu(I), in which the nitrite is coordinated to copper via a nitrogen, as displayed in Figure 4B. We have also explored the second approach by using the computationally optimized nitrite-Cu(II) complex (Figure 4A) as a starting geometry. These calculations found a single oxygen coordination instead. Both single N- and O- coordinations results agree with the theoretical results of Sundararajan.<sup>24</sup> Nevertheless, the single N-coordinated mode has an energy lower by 8.15 kcal/mol. We thus focus on the single N-coordinated nitrite-Cu(I) form because of its lower energy.

**Side-On versus End-On Coordination of NO.** Measurements of crystal structures of nitrite-attached CuNiR agree that nitrite binds to the T2 Cu in a bidentate way via the two oxygen atoms.<sup>8,9</sup> However, the structure of the nitric oxide intermediate remains controversial. On the basis of the earlier investigation of NO attachment to a synthetic mononuclear copper nitrosyl model complex, N-coordination was expected.<sup>42</sup> Surprisingly, experiments<sup>11,12</sup> examining the NO intermediate in CuNiR found a different type of attachment, in which the distances of N and O to copper are equidistant as shown in Figure 5. This arrangement has been termed “side-on”, while the N-coordinated one was named “end-on”. While the first<sup>11</sup> of those studies found the side-on coordination only for the reduced state of the enzyme, which is not relevant for the catalytic process, the second study<sup>12</sup> detected side-on attachment for both oxidized and reduced states. In contrast, an EPR-ENDOR study<sup>25</sup> has yielded EPR parameters consistent

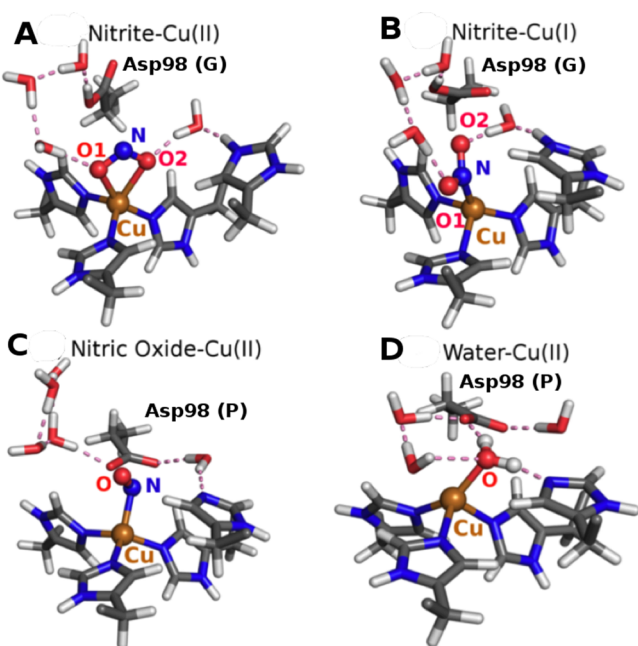


**Figure 4.** Optimized structures of the favorable conformations. (A) Before electron transfer (ET), the nitrite attaches to T2 Cu<sup>2+</sup> and Asp<sup>98</sup> is in the “gatekeeper” position. (B) After ET, the nitrite remains attached to T2 Cu<sup>+</sup> and Asp<sup>98</sup> is still in the “gatekeeper” position. (C) After nitrite reduction, NO coordinates to T2 Cu<sup>2+</sup> and Asp<sup>98</sup> moves to the “proximal” position. (D) After NO release, water coordinates to T2 Cu<sup>2+</sup> and Asp<sup>98</sup> is still in the “proximal” position. The dashed lines show the hydrogen-bonded network. Asp<sup>98</sup> and His<sup>255</sup> are protonated in (A) and (B), and deprotonated in (C) and (D). Only the nearby atoms are displayed for clarity. Letters “G” and “P” denote “gatekeeper” and “proximal” orientations of Asp<sup>98</sup>, respectively.

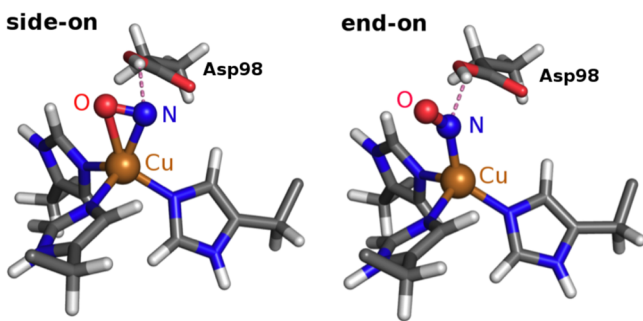


**Figure 5.** Side-on (left) and end-on (right) coordination of nitric oxide at T2 Cu<sup>+</sup>. N–Cu, O–Cu, and N–O distances are 1.96, 2.13, 1.23 Å for side-on (SO) and 1.89, 2.87, 1.19 Å for end-on (EO) configurations. Only the nearby atoms are displayed for clarity.

with an end-on rather than a side-on structure. Nevertheless, the observations of the side-on attachment have attracted considerable attention, since they would have important implications for the mechanism of the catalytic process.

Existing DFT calculations<sup>22–26</sup> have so far only addressed the reduced state of the enzyme. These works have shown that the side-on attachment in Cu(I)-NO is stabilized by a hydrogen bond between NO and Asp<sup>98</sup> along with interactions with Ile<sup>257</sup> and His<sup>255</sup>. These studies have found that the Cu(I)-NO end-on attachment is favored by 3.00–9.91 kcal/mol. Ref 26 has also shown that the steric constraint of the CuNiR active site is an important factor for the side-on coordination. However, so far, it has not been conclusively determined whether the side-on coordination is a part of the catalytic process, since the enzyme is in the oxidized rather than the reduced state when NO attaches.

Our calculations examining the reduced enzyme show that the side-on configuration is only a local minimum, while the end-on configuration is lower in energy by 6.22 kcal/mol. The fully optimized structures of both configurations are displayed in Figure 5. Comparisons of experimental and calculated structures are displayed in Figure S2 (SI) for both side-on and end-on coordinations to Cu(I). While the N–Cu and O–Cu bond lengths are in close agreement with the experiment data, the N–O bond (1.23 Å) is significantly shorter than the observed value of 1.45 Å found in refs 11 and 12. Given that the gas phase value is 1.15 Å, such a bond length is unusually long. In fact, none of the other calculations<sup>22–26</sup> were able to reproduce the experimental value either, and all yielded bond lengths similar to ours. In our attempt to reproduce the experimental bond length, we have varied different computational parameters, including the level of theory (MP2 instead of DFT, details of the MP2 calculation are provided in SI), system size, initial configuration, protonation states of key residues, and oxidation states of the enzyme. Of these, only an extreme reduction of the enzyme, adding two electrons to the reduced form of enzyme, yielded a substantially longer NO bond, 1.35 Å. However, it appears unlikely that such an extreme reduction could take place under experimental conditions. A more likely explanation seems to be disorder in the ligands, which was previously found to affect bond lengths in other metal-NO adducts.<sup>43</sup> Another factor may be the resolution of the X-ray experiment: Of the two works reporting the side-on structure, the one with a higher resolution (0.9–1.1 Å)<sup>12</sup> reports a range of NO distances of 1.25–1.40 Å, where the low end is close to the calculated N–O distance of 1.23 Å. The experiment with

1.3 Å resolution<sup>11</sup> finds all NO bond distances to be around 1.45 Å.

For an oxidized form of CuNiR, which occurs when NO attaches during the catalytic process, our calculations could not find a stable side-on configuration. Starting from the experimental structures, side-on attachments quickly relax to end-on ones. The same is found when the initial structure is set up manually, which leads us to conclude that a side-on configuration is not an energy minimum for the oxidized CuNiR. In the relaxed end-on attachment, the N–Cu and O–Cu bond distances are 1.81 and 2.80 Å, respectively. Comparisons of experimental and calculated structures are displayed in Figure S2 (SI) for the end-on coordination to Cu(II). Because of this finding, our investigation of the catalytic mechanism of CuNiR assumes the end-on attachment of NO.

**Mechanism of Enzymatic Function of CuNiR.** As a prerequisite for the investigation of CuNiR, we first examine the protonation states of key residues, since they cannot be determined in X-ray experiments. On the basis of ref 31, the reaction mechanism needs two protons. However, their origin is not known. There are two residues that can provide protons: Asp<sup>98</sup> and His<sup>255</sup>. In addition, the substrate (nitrite) can already be protonated at the start of the reaction.<sup>11,12</sup> Our calculations find that only the state with both Asp<sup>98</sup> and His<sup>255</sup> protonated gives the expected bidentate oxygen attachment of the substrate,<sup>11,12</sup> suggesting that these two residues are protonated when NO<sub>2</sub><sup>–</sup> attaches.

Another important mechanistic question of CuNiR action is the point at which the electron transfers from the T1 to the T2 copper. Whether this happens before or after the substrate (nitrite) attachment is still being disputed.<sup>44</sup> Our calculations explore the former case, which has been assumed in our two main experimental references.<sup>11,12</sup> The difference between the two cases is the initial attachment of the substrate: if the copper binding site is reduced, the substrate attaches in a single nitrogen coordination, while for the oxidized enzyme the commonly accepted double oxygen coordination mode takes place. Our choice is also consistent with the experimental results of Hough and co-workers,<sup>45</sup> who showed that electron transfer is gated by the attachment of nitrite.

After we have identified the protonation states of the key residues, the conformational changes in Asp<sup>98</sup>, and the point at which the electron transfer occurs, the enzymatic mechanism can be drawn in detail, as shown in Figure 6. It should be noted that given the experimental data of refs 11 and 12, our calculations eliminated alternative possibilities, and the mechanism in Figure 6 is the only one consistent with the experimental data. The eliminated alternative possibilities include (1) only one proton is involved in the reaction, which together with one oxygen from the nitrite produces a hydroxyl instead of a water molecule; (2) two protons are involved with one on either Asp<sup>98</sup> or His<sup>255</sup>, and the other on nitrite; (3) electron transfer (from T1 Cu to T2 Cu) occurs before the nitrite attaches to copper.

The mechanism starts with nitrite attachment to copper, which displaces a water molecule. This is followed by an electron transfer reducing the T2 copper to Cu(I). Next, nitrite reduction occurs, and one oxygen of the nitrite is cleaved and forms a water molecule with protons from Asp<sup>98</sup> and His<sup>255</sup>, with the second proton being bridged by crystallographic water. The produced water molecule forms a hydrogen bond with Asp<sup>98</sup>. The nitric oxide is then released, and the water binds to

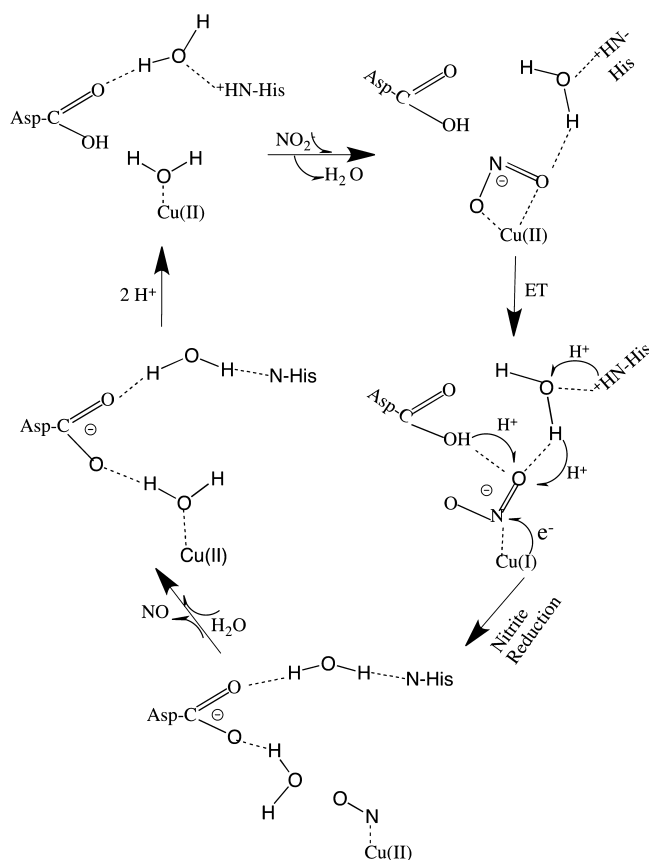


Figure 6. Scheme of the enzymatic mechanism.

copper. At the end, the enzyme needs to be reprotonated to return to the initial state.

After determining all the key steps in the enzymatic mechanism, we use NEB calculations to find full atomic geometries, transition states, and activation barriers. The energy barriers gauge the feasibility of the mechanism because processes with barriers in excess of 30 kcal/mol are unlikely to take place under normal conditions.

The NEB calculations have examined the mechanism in three steps: (i) nitrite attachment, (ii) nitrite reduction, and (iii) nitric oxide release. The overall energy profile is shown in Figure 7, where the NEB image number denotes intermediate structures between initial and final states (it can also be thought of as the collective reaction coordinate connecting the initial and final states). The blue solid line is the energy landscape of the three subprocesses with flexible Asp<sup>98</sup>, which changes conformations during the reaction. The red dashed line in the middle panel is the energy profile for nitrite reduction with Asp<sup>98</sup> staying in "proximal" position (static Asp<sup>98</sup>), i.e., no switch between the two conformations. In the middle panel, for the two initial states, the energy difference is 8.76 kcal/mol (Table 1, second row), as Asp<sup>98</sup> is in the proximal position in static case and in the gatekeeper position in flexible case. For the two final states, the energies are very close, as Asp<sup>98</sup> is in the proximal position in both cases, with the minor difference resulting from orientations of the water molecules (see image 9 in Figures S4 and S5 for details). The initial, final, and transition state structures for each subprocess in the flexible case are displayed in Figure 8. A larger view of the three structures in each process is displayed in Figure S3 (SI), where the distances are shown in Å.

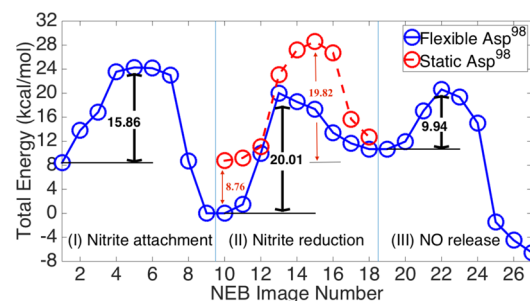
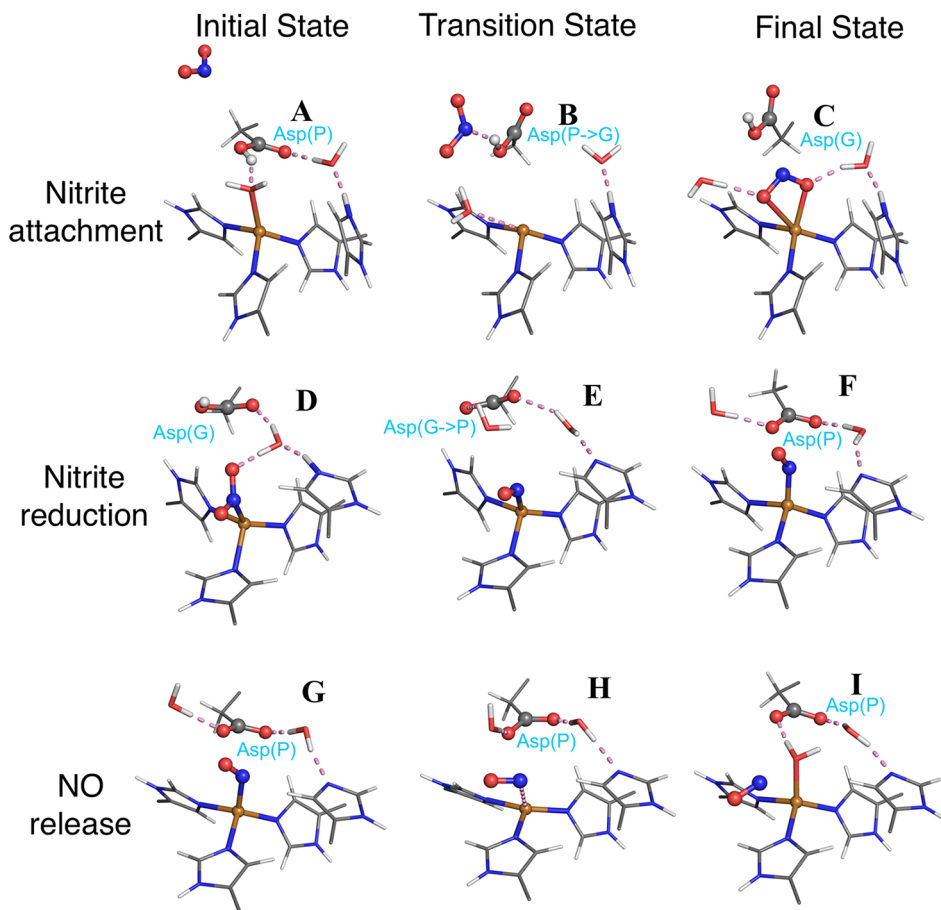


Figure 7. Energy landscape of the catalytic reaction. The panels (II) and (III) are shifted vertically by 130.44 kcal/mol to account for electron transfer (not included in the calculations) and substrate coordination change following the transfer (see text). The blue solid line is the energy landscape of the three subprocesses with flexible Asp<sup>98</sup>, which changes conformations during the reaction. The red dashed line in the middle panel is the energy profile for nitrite reduction with Asp<sup>98</sup> staying in the "proximal" position (static Asp<sup>98</sup>), i.e., no switch between the two conformations. In the middle panel, for the two initial states, the energy difference is 8.76 kcal/mol (Table 1, second row), as Asp<sup>98</sup> is in the proximal position in the static case and in the gatekeeper position in the flexible case. For the two final states, the energies are very close as Asp<sup>98</sup> is in the proximal position in both cases, with the minor difference due to orientations of water molecules (see image 9 in Figure S4 and S5 for details). The NEB image number denotes intermediate structures between the initial and final states.

During the nitrite attachment (as displayed in Figure 8A–C), Asp<sup>98</sup> moves from the proximal position to the gatekeeper position, while the resting state water is replaced by nitrite. The activation energy of this process is 15.86 kcal/mol. In the transition state (Figure 8B), the water–Cu distance is extended, while the nitrite forms a hydrogen bond with the carboxyl hydrogen in Asp<sup>98</sup>. At the end of this process, the nitrite is doubly O-coordinated to the T2 Cu (II), as shown in Figure 8C.

This is followed by electron transfer from the T1 copper to the T2 copper. The electron is provided by a physiological electron donor<sup>2</sup> and is transferred to the T2 Cu via Cys-His bridge. The electron transfer process is not a part of our calculations. It reduces the T2 copper to Cu(I), which in turn leads to a change in nitrite attachment mode from bidentate oxygen coordination (Figure 8C) to monodentate nitrogen coordination (Figure 8D). There is no energy barrier for this change once ET takes place. Because of ET, the structures of final state of the nitrite attachment, Figure 8C, and the initial state of the next process (nitrite reduction, Figure 8D) differ.

In the nitrite reduction process, a proton is transferred to one of the nitrite's oxygens from His<sup>255</sup> via a proton bridge formed by a crystallographic water molecule between Asp<sup>98</sup> and His<sup>255</sup>. As a result, the oxygen's bond to the nitrite becomes extended and weaker. Next, the second proton is transferred to the oxygen forming a water molecule, which cleaves from the nitrite. The second proton transfer and the cleavage proceed simultaneously. Initial, transition, and final states of the nitrite reduction are displayed in Figure 8D–F. Detailed structures for all the steps along the minimum energy pathway are shown in Figure S4 (SI). During this process, the side chain of Asp<sup>98</sup> moves from the gatekeeper to the proximal conformation. In the transition state (Figure 8E), a water molecule forms a hydrogen bond to Asp<sup>98</sup> and NO is nitrogen coordinated (end-on) to the T2 copper. Such attachment can exist in two possible electronic structure configurations: Cu(I)-NO<sup>+</sup> and



**Figure 8.** Minimum energy pathways (MEP) with initial, transition, and final states for the three processes. Only the atoms near the T2 Cu are displayed for clarity. Hydrogen bonded networks are shown by dashed lines. Letters “G” and “P” denote “gatekeeper” and “proximal” orientations of Asp<sup>98</sup>, respectively.

Cu(II)-NO. The calculations show that the former form is preferred in energy. The activation energy of the reduction process is 20.01 kcal/mol. Overall, as shown in Figure 7, nitrite reduction is an endothermic process requiring 12 kcal/mol. This agrees well with the experimental estimate of 15 kcal/mol.<sup>46</sup>

Finally, the nitric oxide is released from T2 Cu (II) and a water is bound to the copper as displayed in Figure 8G–I. The enzyme returns to the resting state with Asp<sup>98</sup> and His<sup>255</sup> deprotonated (Figure 8I). The activation energy of the release process is 9.94 kcal/mol. To fully recover the resting state, Asp<sup>98</sup> and His<sup>255</sup> need to be reprotonated, but this process has not been included in our calculations.

The process investigated above assumed that Asp<sup>98</sup>’s side chain switches between proximal and gatekeeper positions. However, this was only reported in one experimental study,<sup>12</sup> and thus we also examine a catalytic process in which Asp<sup>98</sup> stays in the proximal position. Specifically, we repeat the NEB calculation for the second process, nitrite reduction, with Asp<sup>98</sup> in the proximal position. The energy profile is displayed as a dashed line in the middle panel of Figure 7. The comparison shows that both cases have very similar energy barriers—20.01 kcal/mol for switching and 19.82 kcal/mol without switching. Also, the reduction process proceeds in same way for both cases: First, His<sup>255</sup> transfers a proton to one of the oxygens of the nitrite causing extension of its bond to the nitrogen. Next, a proton transfer from Asp<sup>98</sup> to the same oxygen forms a water

molecule which is simultaneously cleaved from the nitrite, leaving NO attached to the copper center. A detailed sequence of all the steps along the minimum energy pathway is displayed in Figure S5 (SI). Overall, these results show that the Asp<sup>98</sup> position switching does not have a significant effect on the nitrite reduction barrier.

While our calculations assume that the ET takes place after the substrate attachment, it should be noted that the nitrite reduction and the NO release subprocesses are valid for both cases. If the enzyme is reduced prior to the substrate attachment, the attachment process would be different (our calculations would suggest that the nitrite attaches in the N-coordination as in Figure 4B), but the nitrite reduction and the product release subprocesses would be the same.

The nitrite reduction in CuNiR was previously investigated<sup>31</sup> using saddle point calculations. This work used experimental data from a different species (*Alcaligenes xylosoxidans*<sup>47</sup>) and therefore used a different model of the binding site and the key intermediate. Because of this, the details of the catalytic process are different, and energy barriers are not directly comparable (they found an energy barrier of 11.6 kcal/mol). Despite these differences, an agreement is found in the sequence of proton transfers and the fact that the N–O bond breakage occurs simultaneously with the second proton transfer.

We have also evaluated the effect of solvent on the activation barriers by adding 500 explicit water molecules surrounding our model cluster. The positions of the waters were optimized

using PWScf. The results show that the solvation only has a minor effect because the activation barriers change by 4 kcal/mol or less for all the processes studied in this work.

## ■ DISCUSSION

**Electron-Transfer-Induced Change of the Coordination of Nitrite.** An important aspect of the CuNiR mechanism is the substrate coordination change during the reaction. Initially, the substrate (nitrite) is doubly oxygen coordinated, while the product (NO) is nitrogen coordinated. How this change occurs is not known. Experiments that found the side-on attachment of the NO have posited that the coordination change proceeds via the side-on intermediate.

However, our calculations based on the initial experimental structures find a different mechanism for the coordination change. The main factor is the reduction of the T2 copper (caused by an electron transfer from the Type 1 copper, which receives an electron from a physiological electron donor).<sup>2</sup> Our calculations start with the experimental structure of the substrate-bound enzyme, in which substrate is, as expected, doubly oxygen coordinated (Figure 8C). The calculations show that this configuration has the lowest energy and thus is stable. However, when the charge state of the T2 copper changes from Cu(II) to Cu(I), corresponding to the reduction of the enzyme, double oxygen coordination is no longer a minimum and the system relaxes to N-coordination (Figure 8D) without encountering an energy barrier. Therefore, the calculations predict that the coordination change takes place before the oxygen is cleaved from the substrate and that the reduction of the enzyme is the trigger causing the coordination change.

**Conformational Change of Asp<sup>98</sup> During the Enzymatic Function.** Asp<sup>98</sup> is in either the “gatekeeper” configuration or the “proximal” configuration at different stages of its function, as shown in Figure 8. The letter “G” in Figure 8 represents the “gatekeeper” orientation, while the letter “P” stands for the “proximal” orientation. In the resting state, the “proximal” position is energetically favorable when a water molecule binds to the T2 copper. However, upon the attachment of nitrite, the “gatekeeper” configuration becomes preferred.

The binding of nitrite is then followed by an electron transfer from T1 Cu to T2 Cu. It causes a reduction of the charge state of the T2 copper from Cu(II) to Cu(I). At that point, the “gatekeeper” position is still favored. However, compared to the structure before, the Asp<sup>98</sup> is now closer to the binding site. This is shown in Figure 4A,B. Therefore, the effect of electron transfer is not only changing the coordination mode of the nitrite, but also bringing the Asp<sup>98</sup> in the “gatekeeper” position closer to the T2 copper site.

Next in the nitrite reduction process, an oxygen is cleaved from the nitrite, resulting in a N-coordinated (end-on) nitric oxide bound to the T2 Cu. At this point, the “proximal” position of Asp<sup>98</sup> is preferred. During the final nitric oxide release process, the “proximal” position attachments are favored for both the nitric oxide and the water molecule at the binding site.

Our calculations also considered the case in which the Asp<sup>98</sup> stays in the proximal position during the entire catalytic process. It is found that this has no significant influence on the activation barrier or the mechanism of the nitrite reduction process.

## ■ CONCLUSION

We have explored the enzymatic function of copper-containing nitrite reductase and found that only a single mechanism is consistent with the structural data available for key intermediates. The entire mechanism has been mapped out in atomistic detail, along with transition states, energy barriers, and the rate-limiting step. Several important aspects of the process have been resolved, including the origins of the two protons needed for the reaction. The roles of proposed Asp<sup>98</sup>’s structural changes have been investigated, and we find that while they play role in the attachment of the substrate, they do not affect the activation energy and reaction pathways on the nitrite reduction process. We also find that the previously observed side-on coordination of the NO intermediate does not occur during the normal function of CuNiR. These results provide important insights and improve our understanding of the functioning of this enzyme. Two aspects were not included in this work: electron transfer from the T1 copper and reprotonation of Asp<sup>98</sup> and His<sup>255</sup>.

CuNiR has the potential for use in environmental remediation and removal of excess nitrogen from aquatic environments. We find that nitrite reduction and attachment are the main rate limiting steps with energy barriers of 20.05 and 15.44 kcal/mol, respectively. The former barrier may be reduced by optimizing the T2 Cu binding site, while the latter can be decreased by improving the substrate channel leading to the catalytic site, but these are beyond the scope of this work.

## ■ ASSOCIATED CONTENT

### Supporting Information

Comparisons of experimental and calculated structures, larger views of the NEB structures shown in Figure 8 in the paper, full NEB pathways of the nitrite reduction process for both flexible and static Asp<sup>98</sup>, the optimized structures of different enzymatic states in the same view, and detailed lists of residues forming the walls of the nitrite and NO channels. This material is available free of charge via the Internet at <http://pubs.acs.org>.

## ■ AUTHOR INFORMATION

### Corresponding Authors

\*(M.H.) E-mail: Tel: 919-513-0612. Fax: 919-513-4804. E-mail: mhodak@ncsu.edu.

\*(J.B.) E-mail: Tel: 919-515-3126. Fax: 919-513-4804. E-mail: bernholc@ncsu.edu.

### Funding

This work was supported by DOE DE-FG02-98ER45685, with petascale code development supported by NSF OCI-0749320 and ACI-1339844. The supercomputer time was provided by NSF Grant OCI-1036215 at the National Center for Supercomputing Applications and by DOE at the National Center for Computational Sciences at ORNL.

### Notes

The authors declare no competing financial interest.

## ■ REFERENCES

- (1) Vitousek, P., Aber, J., Howarth, R., Likens, G., Matson, P., Schindler, D., Schlesinger, W., and Tilman, D. (1997) Human alteration of the global nitrogen cycle: sources and consequences. *Ecol. Appl.* 7, 737–750.
- (2) Averill, B. (1996) Dissimilatory nitrite and nitric oxide reductases. *Chem. Rev.* 96, 2951–2964.
- (3) MacPherson, I., and Murphy, M. (2007) Type-2 copper-containing enzymes. *Cell. Mol. Life Sci.* 64, 2887–2899.

(4) Fülöp, V., Moir, J., Ferguson, S., and Hajdu, J. (1995) The anatomy of a bifunctional enzyme: Structural basis for reduction of oxygen to water and synthesis of nitric oxide by cytochrome Cd(1). *Cell* 81, 369–377.

(5) Libby, E., and Averill, B. (1992) Evidence that the type 2 copper centers are the site of nitrite reduction by *Achromobacter cycloclastes* nitrite reductase. *Biochem. Biophys. Res. Commun.* 187, 1529–1535.

(6) Abraham, Z., Lowe, D., and Smith, B. (1993) Purification and characterization of the dissimilatory nitrite reductase from *Alcaligenes xylosoxidans* subsp. *xylosoxidans* (NCIMB 11015): evidence for the presence of both type 1 and type 2 copper centres. *Biochem. J.* 295, 587.

(7) Kukimoto, M., Nishiyama, M., Murphy, M., Turley, S., Adman, E., Horinouchi, S., and Beppu, T. (1994) X-ray structure and site-directed mutagenesis of a nitrite reductase from *Alcaligenes faecalis* S-6: roles of two copper atoms in nitrite reduction. *Biochemistry (N.Y.)* 33, 5246–5252.

(8) Murphy, M., Turley, S., and Adman, E. (1997) Structure of nitrite bound to copper-containing nitrite reductase from *Alcaligenes faecalis*. *J. Biol. Chem.* 272, 28455.

(9) Boulanger, M., and Murphy, M. (2001) Alternate substrate binding modes to two mutant (D98N and H255N) forms of nitrite reductase from *Alcaligenes faecalis* S-6: structural model of a transient catalytic intermediate. *Biochemistry (N.Y.)* 40, 9132–9141.

(10) Tocheva, E., Eltis, L., and Murphy, M. (2008) Conserved Active Site Residues Limit Inhibition of a Copper-Containing Nitrite Reductase by Small Molecules. *Biochemistry (N.Y.)* 47, 4452–4460.

(11) Tocheva, E. I., Rosell, F. I., Mauk, A. G., and Murphy, M. E. P. (2004) Side-On Copper-Nitrosyl Coordination by Nitrite Reductase. *Science* 304, 867–870.

(12) Antonyuk, S. V., Strange, R. W., Sawers, G., Eady, R. R., and Hasnain, S. S. (2005) Atomic resolution structures of resting-state, substrate- and product-complexed Cu-nitrite reductase provide insight into catalytic mechanism. *Proc. Natl. Acad. Sci. U. S. A.* 102, 12041–12046.

(13) Tocheva, E., Rosell, F., Mauk, A., and Murphy, M. (2007) Stable copper-nitrosyl formation by nitrite reductase in either oxidation state. *Biochemistry (N.Y.)* 46, 12366–12374.

(14) Jacobson, F., Pistorius, A., Farkas, D., De Grip, W., Hansson, Ö., Sjölin, L., and Neutze, R. (2007) pH dependence of copper geometry, reduction potential, and nitrite affinity in nitrite reductase. *J. Biol. Chem.* 282, 6347–6355.

(15) Yokoyama, H., Yamaguchi, K., Sugimoto, M., and Suzuki, S. (2005) CuI and CuII Complexes Containing Nitrite and Tridentate Aromatic Amine Ligand as Models for the Substrate-Binding Type-2 Cu Site of Nitrite Reductase. *Eur. J. Inorg. Chem.* 2005, 1435–1441.

(16) Usov, O., Sun, Y., Grigoryants, V., Shapleigh, J., and Scholes, C. (2006) EPR-ENDOR of the Cu (I) NO complex of nitrite reductase. *J. Am. Chem. Soc.* 128, 13102–13111.

(17) Lehnert, N., Cornelissen, U., Neese, F., Ono, T., Noguchi, Y., Okamoto, K., and Fujisawa, K. (2007) Synthesis and spectroscopic characterization of copper (II)-nitrito complexes with hydrotris (pyrazolyl) borate and related coligands. *Inorg. Chem.* 46, 3916–3933.

(18) Boulanger, M., Kukimoto, M., Nishiyama, M., Horinouchi, S., and Murphy, M. (2000) Catalytic roles for two water bridged residues (Asp-98 and His-255) in the active site of copper-containing nitrite reductase. *J. Biol. Chem.* 275, 23957–23964.

(19) Kataoka, K., Furusawa, H., Takagi, K., Yamaguchi, K., and Suzuki, S. (2000) Functional Analysis of Conserved Aspartate and Histidine Residues Located Around the Type 2 Copper Site of Copper-Containing Nitrite Reductase. *J. Biochem.* 127, 345–350.

(20) Prudêncio, M., Eady, R., and Sawers, G. (1999) The Blue Copper-Containing Nitrite Reductase from *Alcaligenes xylosoxidans*: Cloning of the *nirA*Gene and Characterization of the Recombinant Enzyme. *J. Bacteriol.* 181, 2323–2329.

(21) Zhang, H., Boulanger, M., Mauk, A., and Murphy, M. (2000) Carbon monoxide binding to copper-containing nitrite reductase from *Alcaligenes faecalis*. *J. Phys. Chem. B* 104, 10738–10742.

(22) Silaghi-Dumitrescu, R. (2006) Copper-containing nitrite reductase: A DFT study of nitrite and nitric oxide adducts. *J. Inorg. Biochem.* 100, 396–402.

(23) Ghosh, S., Dey, A., Usov, O., Sun, Y., Grigoryants, V., Scholes, C., and Solomon, E. (2007) Resolution of the spectroscopy versus crystallography issue for NO intermediates of nitrite reductase from *rhodobacter sphaeroides*. *J. Am. Chem. Soc.* 129, 10310–10311.

(24) Sundararajan, M., Hillier, I., and Burton, N. (2007) Mechanism of nitrite reduction at T2Cu centers: Electronic structure calculations of catalysis by copper nitrite reductase and by synthetic model compounds. *J. Phys. Chem. B* 111, 5511–5517.

(25) Periyasamy, G., Sundararajan, M., Hillier, I., Burton, N., and McDouall, J. (2007) The binding of nitric oxide at the Cu (I) site of copper nitrite reductase and of inorganic models: DFT calculations of the energetics and EPR parameters of side-on and end-on structures. *Phys. Chem. Chem. Phys.* 9, 2498–2506.

(26) Merkle, A., and Lehnert, N. (2009) The Side-On Copper (I) Nitrosyl Geometry in Copper Nitrite Reductase Is Due to Steric Interactions with Isoleucine-257. *Inorg. Chem.* 48, 11504–11506.

(27) Hohenberg, P., and Kohn, W. (1964) Inhomogeneous Electron Gas. *Phys. Rev.* 136, B864–B871.

(28) Kohn, W., and Sham, L. J. (1965) Self-Consistent Equations Including Exchange and Correlation Effects. *Phys. Rev.* 140, A1133–A1138.

(29) Henkelman, G., and Jónsson, H. (2000) Improved tangent estimate in the nudged elastic band method for finding minimum energy paths and saddle points. *J. Chem. Phys.* 113, 9978.

(30) Henkelman, G., Uberuaga, B., and Jónsson, H. (2000) A climbing image nudged elastic band method for finding saddle points and minimum energy paths. *J. Chem. Phys.* 113, 9901.

(31) De Marothy, S., Blomberg, M., and Siegbahn, P. (2007) Elucidating the mechanism for the reduction of nitrite by copper nitrite reductaseA contribution from quantum chemical studies. *J. Comput. Chem.* 28, 528–539.

(32) Wirstam, M., Blomberg, M., and Siegbahn, P. (1999) Reaction mechanism of compound I formation in heme peroxidases: a density functional theory study. *J. Am. Chem. Soc.* 121, 10178–10185.

(33) Mulholland, A. (2005) Modelling enzyme reaction mechanisms, specificity and catalysis. *Drug Discovery Today* 10, 1393–1402.

(34) Senn, H., and Thiel, W. (2007) QM/MM studies of enzymes. *Curr. Opin. Chem. Biol.* 11, 182–187.

(35) Siegbahn, P., and Blomberg, M. (1999) Density functional theory of biologically relevant metal centers. *Annu. Rev. Phys. Chem.* 50, 221–249.

(36) Briggs, E., Sullivan, D., and Bernholc, J. (1995) Large-scale electronic-structure calculations with multigrid acceleration. *Phys. Rev. B* 52, 5471–5474.

(37) Briggs, E., Sullivan, D., and Bernholc, J. (1996) Real-space multigrid-based approach to large-scale electronic structure calculations. *Phys. Rev. B* 54, 14362.

(38) Hodak, M., Wang, S., Lu, W., and Bernholc, J. (2007) Implementation of ultrasoft pseudopotentials in large-scale grid-based electronic structure calculations. *Phys. Rev. B* 76, 085108.

(39) Giannozzi, P., et al. (2009) QUANTUM ESPRESSO: a modular and open-source software project for quantum simulations of materials. *J. Phys: Condens Matter* 21, 395502.

(40) Petřek, M., Otyepka, M., Banáš, P., Košinová, P., Koča, J., and Damborský, J. (2006) CAVER: a new tool to explore routes from protein clefts, pockets and cavities. *BMC Bioinformatics* 7, 316.

(41) *The PyMOL Molecular Graphics System*, Version 1.3r1; Schrödinger, LLC: Portland, OR.

(42) Ruggiero, C. E., Carrier, S. M., Antholine, W. E., Whittaker, J. W., Cramer, C. J., and Tolman, W. B. (1993) Synthesis and structural and spectroscopic characterization of mononuclear copper nitrosyl complexes: Models for nitric oxide adducts of copper proteins and copper-exchanged zeolites. *J. Am. Chem. Soc.* 115, 11285–11298.

(43) Wyllie, G. R., and Scheidt, W. R. (2002) Solid-state structures of metalloporphyrin NO<sub>x</sub> compounds. *Chem. Rev.* 102, 1067–1089.

(44) Wijma, H., Jeuken, L., Verbeet, M., Armstrong, F., and Canters, G. (2006) A random-sequential mechanism for nitrite binding and active site reduction in copper-containing nitrite reductase. *J. Biol. Chem.* 281, 16340–16346.

(45) Hough, M. A., Antonyuk, S. V., Strange, R. W., Eady, R. R., and Hasnain, S. S. (2008) Crystallography with online optical and X-ray absorption spectroscopies demonstrates an ordered mechanism in copper nitrite reductase. *J. Mol. Biol.* 378, 353–361.

(46) Zhao, Y., Lukyanov, D. A., Toropov, Y. V., Wu, K., Shapleigh, J. P., and Scholes, C. P. (2002) Catalytic function and local proton structure at the type 2 copper of nitrite reductase: the correlation of enzymatic pH dependence, conserved residues, and proton hyperfine structure. *Biochemistry (N.Y.)* 41, 7464–7474.

(47) Ellis, M. J., Dodd, F. E., Sawers, G., Eady, R. R., and Hasnain, S. S. (2003) Atomic Resolution Structures of Native Copper Nitrite Reductase from *Alcaligenes xylosoxidans* and the Active Site Mutant Asp92Glu. *J. Mol. Biol.* 328, 429–438.